

Genetic analysis of hemopoietic cell cycling in mice suggests its involvement in organismal life span

GERALD DE HAAN*[†] AND GARY VAN ZANT*¹

*Blood and Marrow Transplant Program, Division of Hematology/Oncology, University of Kentucky Medical Center, Lexington, Kentucky 40536-0093, USA; and [†]Department of Physiological Chemistry, University of Groningen, Groningen, The Netherlands

ABSTRACT Normal somatic cells undergo replicative senescence *in vitro* but the significance of this process in organismic aging remains controversial. We have shown previously that hemopoietic stem cells of common inbred strains of mice vary widely in cycling activity and that this parameter is inversely correlated with strain-dependent mean life span. To assess whether cell cycling and life span are causally related, we searched for quantitative trait loci (QTLs) that contributed to variation of these traits in BXH and BXD recombinant inbred mice. Two QTLs, mapping to exactly the same intervals on chromosomes 7 and 11, were identified that were associated with variation of both cell cycling and life span. The locus on chromosome 11 mapped to the cytokine cluster, a segment that shows synteny with human chromosome 5q, in which deletions are strongly associated with myelodysplastic syndrome. These data indicate that steady-state cell turn-over, here measured in hemopoietic progenitor cells, may have a significant effect on the mean life span of mammals. de Haan, G., Van Zant, G. Genetic analysis of hemopoietic cell cycling in mice suggests its involvement in organismal life span. *FASEB J.* 13, 707–713 (1999)

Key Words: stem cells · longevity · cell proliferation · aging · quantitative trait locus

MATURE BLOOD CELLS in the circulation are derived from primitive hemopoietic stem cells residing in the bone marrow. A hierarchy of distinct stem cell subsets can be recognized in which the most primitive, long-term repopulating cells have a very low fraction of cells in S-phase, whereas more committed, but still pluripotent, progenitors have a much higher proliferative activity (1–3). However, we have shown that the number of progenitor cells in S-phase varies widely between different inbred strains of mice (4–6); it is inversely correlated with mean mouse life span and decreases during aging in a strain-dependent fashion (5, 6). In addition, we demonstrated in chimeric mice, constructed by aggregating embryos of strains with intrinsic differences in hemopoietic stem cell cycling, that the more proliferative stem

cell population (DBA/2) underwent replicative senescence after ~1.5–2 years (about the normal life span of this strain), leaving all subsequent blood cell formation in the chimera to the coexistent, largely quiescent stem cells of the long-lived genotype (C57BL/6) (7). Others have shown that the proliferative potential of individual human hemopoietic stem cells decreases greatly during development from fetal liver to cord blood to adult bone marrow, and this is inversely correlated with the mean telomere length of such cell populations (8). Recent clinical findings have shown that accelerated telomere shortening occurs after stem cell transplantation where the relatively few stem cells present in the graft are subjected to intense replicative stress during engraftment (9, 10). These observations on the kinetics of blood cell formation were reminiscent of the data originally presented by Hayflick et al. (11) on the kinetics of fibroblast growth. It was proposed that normal somatic cells have an upper limit to replication, and once this is reached, proliferation decreases and cells ultimately senesce. Recently, it has been shown that telomeres play a role in this process, since expression of telomerase in cells that normally do not express this enzyme delays or prevents senescence (12). It has been suggested that this cellular mitotic clock also sets the limits of organismic life span, since there is an inverse correlation between the proliferation potential of fibroblasts and the age of the donor (13). Collectively, these data indicate a potential relationship between cell proliferation and *in vivo* aging.

To demonstrate that cell proliferation is indeed associated with organismic life span, genes that play a role in both processes have to be identified. As a first step toward this goal, we searched for quantitative trait loci (QTLs)² that contribute to hemopoietic

¹ Correspondence: Blood and Marrow Transplant Program, Division of Hematology/Oncology, 800 Rose Street, University of Kentucky Medical Center, Lexington, KY 40536-0093, USA. E-mail: gvzant1@pop.uky.edu

² Abbreviations: CAFC, cobblestone area-forming cell; QTLs, quantitative trait loci; *Scp1*, stem cell proliferation 1 locus on chromosome 7; *Scp2*, locus on chromosome 11; *Scp3*, locus on chromosome 10 mapped in the BXH set.

progenitor cell cycling and mouse life span in BXD and BXH recombinant inbred mice. These genetically mosaic mice are derived from C57BL/6 (low cycling stem cells, long life span) and DBA/2 or C3H/He mice (high cycling stem cells, short life span). Typing these strains for a phenotype of interest may result in a map position harboring the gene that causes the phenotypic variation between the two strains. We demonstrate a strong negative correlation between mouse life span and stem cell cycling in BXD mice, and report the chromosomal map position of two loci, mapping to the same intervals on chromosomes 7 and 11, that were associated with both stem cell cycling and mouse life span. Independent confirmation of the involvement of the locus on chromosome 11 was obtained from the evaluation of BXH mice.

MATERIALS AND METHODS

Mice

Female C57BL/6J, DBA/2J, C3H/HeJ and recombinant inbred BXD/Ty and BXH/Ty mice were purchased from The Jackson Laboratory (Bar Harbor, Maine) and were used at an age of 6-8 wk. Mice were kept in microisolators and were fed sterilized food and water.

Bone marrow cells were flushed from femora obtained from three mice, pooled, and used in the cobblestone area-forming cell (CAFC) assay.

CAFC assay

The CAFC assay, as described by Ploemacher et al. (14), was slightly modified, as published earlier (15). This *in vitro* assay allows quantification of primitive hemopoietic cell subsets of various developmental stages. Cells of the stromal cell line FBMD-1 (16) were seeded in 96-wells plates (Costar, Cambridge, Mass.) in Dulbecco' modified Eagle's medium containing L-glutamine (Life Technologies, Grand Island, N.Y.), supplemented with 5% horse serum and 15% fetal bovine serum (both from Life Technologies), 10^{-4} mol/l β -mercaptoethanol, 10^{-5} mol/l hydrocortisone (Sigma, St Louis, Mo.), 80 U/ml penicillin and 80 μ g/ml streptomycin (both from Life Technologies), and 25 mmol/l NaHCO_3 . Plates were incubated at 33°C in 5% CO_2 and used 10-14 days after seeding. Bone marrow cells were harvested from the mice and a nucleated cell count was performed. To measure the percentage of cells in the S-phase of the cell cycle, we used a hydroxyurea suicide technique, as described previously (5). To this end, two identical samples were diluted to a concentration of 1×10^7 cells/ml. Hydroxyurea (Sigma) was added to one sample at a concentration of 200 μ g/ml and both samples were incubated at 33°C for 1 h. After incubation, both cell suspensions were washed and a nucleated cell count was performed again. Based on this cell count, the CAFC assay was initiated. Bone marrow cells were seeded on the stromal layer in six dilutions, each cell concentration threefold apart (81,000 cells/well being the highest cell concentration, 333 cells/well the lowest). At this time the medium was switched from 5% horse serum and 15% fetal bovine serum to 20% horse serum. For each cell dilution, 40 replicate wells were used. After 1 wk, all wells were evaluated for the presence or

absence of cobblestone areas, defined as colonies of at least five small nonrefractile cells that grow underneath the stromal cells. Colonies scored after 7 days (i.e., CAFC day 7) have been shown to be derived from pluripotent progenitor cells (3, 17). The fraction of cells killed by hydroxyurea was calculated by dividing the estimated CAFC frequency in the hydroxyurea-treated cell suspension by the control value.

Linkage analysis using BXD RI strains

The percentage of CAFC day 7 in S-phase was calculated as described above, and the strain distribution pattern was used to search genome-wide for QTLs that affect the cycling of this cell stage. This was done by entering the values for all 26 BXD strains into the software program MapManager QT (b15) (18), which computes regression statistics between variation in phenotype and variation in alleles at loci that have already been mapped. At present, some 1700 loci have been mapped in the BXD strains. Similarly, mean life span data for the BXD strains obtained from a study published by Gelman et al. (19) were used to search for QTLs associated with mean life span.

Confirmation of linkage using BXH RI strains

We tested all 12 BXH RI strains for progenitor cell cycling in a manner similar to that described above. After an initial genome-wide screen, *Iapls2-37* on chromosome 10 was found to be linked to the trait. Next, a composite interval mapping strategy was used to search for additional loci with modifying effects on cell cycling. This was done as recently described (20), by performing a second genome-wide search, but now controlling for *Iapls2-37*. Thus, an analysis is conducted to search for loci to explain remaining variation not accounted for by the primary QTL (i.e., *Iapls2-37*). To assess the effects of such secondary loci on the primary QTL, the interval mapping procedure on chromosome 10 was repeated by correcting for these modifiers.

Linkage statistics

To establish criteria for suggestive and significant linkage (21), a permutation test was performed using MapManager QT (1000 permutations at 1 cM intervals (22)). This test compares the peak LOD score obtained for a given data set with the peak LOD scores obtained for 1000 random permutations of the same data set (20). To assess genome-wide significance, point-wise probabilities (*P*) for both RI sets for the same interval were pooled using Fisher's equation: $\chi^2 = -2(\ln_{\text{pBXD}} + \ln_{\text{pBXH}})$, with 4 degrees of freedom (20).

RESULTS

Analysis of variation in hemopoietic progenitor cell cycling in BXD recombinant inbred strains

The percentage of CAFC day 7 in S-phase among the BXD strains ranged from undetectable to ~60% of the population (Fig. 1). Some strains (BXD 9, 19, 20, 25, 30) had fewer cells in S-phase than parental C57BL/6, and conversely, several strains (BXD 1, 5, 6, 11, 16, 21, 31, 32) had more cells in S-phase than did DBA/2. Since no mendelian distribution was observed, it was clear that the variation in progenitor cell cycling between C57BL/6 and DBA/2 is caused

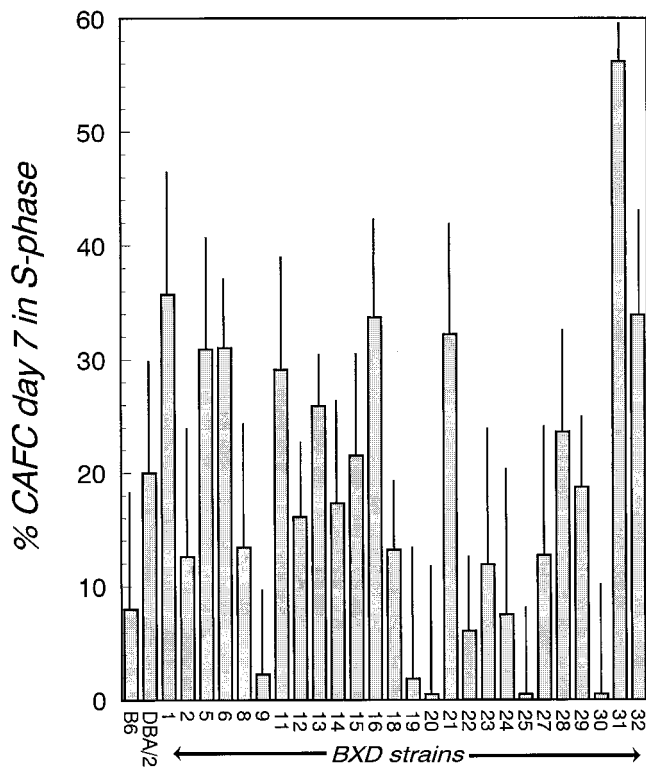


Figure 1. Strain distribution pattern for CAFC day 7 cycling in 26 BXD and parental C57BL/6 (B6) and DBA/2 strains. Bars indicate standard error of the mean. Note that many strains have a smaller or larger population of CAFC day 7 in S-phase than the parental strains.

by multiple, quantitative loci. The extreme differences between ‘outlier’ BXD strains probably results from the random shuffling of different combinations of B6 and DBA alleles that affect cell cycling, so that some strains inherit all the low cycling alleles and other strains inherit all the high cycling alleles. It is also apparent that B6 mice must contain some alleles associated with high cycling that are masked by more dominant low cycling alleles (otherwise strains that have a lower cycling than B6 would not have been found); conversely, DBA mice must contain some low cycling alleles.

Hemopoietic progenitor cell cycling is inversely correlated with mean mouse life span

Our data as presented in Fig. 1 were compared with data obtained by Gelman et al. (19). In this study, life span measurements of 22 BXD strains (10–20 mice per strain) were performed under carefully controlled housing conditions. For example, sentinel animals were present at all times to monitor for microbial pathogens. Histological necropsies revealed a wide range of death causes without any clear patterns. **Figure 2** shows that, in young BXD mice, progenitor cell cycling and mean strain life span were significantly inversely correlated ($P=0.0093$), as

we previously found in a survey of eight commonly used inbred strains (6). Approximately 30% of the variation in mean life span could be explained, and indeed predicted, by differences in cycling ($r^2 = 0.29$).

Mapping of loci associated with progenitor cell cycling and mouse life span

The strain distribution patterns for progenitor cell cycling and life span as shown in Figs. 1 and 2 were used to search for QTLs most strongly associated with these traits using MapManager QT (b15) software (18). A genome-wide search for linkage with progenitor cell cycling revealed four putative loci; one major QTL on chromosome 11, reaching a genome-wide threshold required for suggestive linkage (21, 22), and three weaker ones on chromosomes 4, 7, and 9 (**Table 1**). Similarly, the data of Gelman et al. (19) were used to search for QTLs

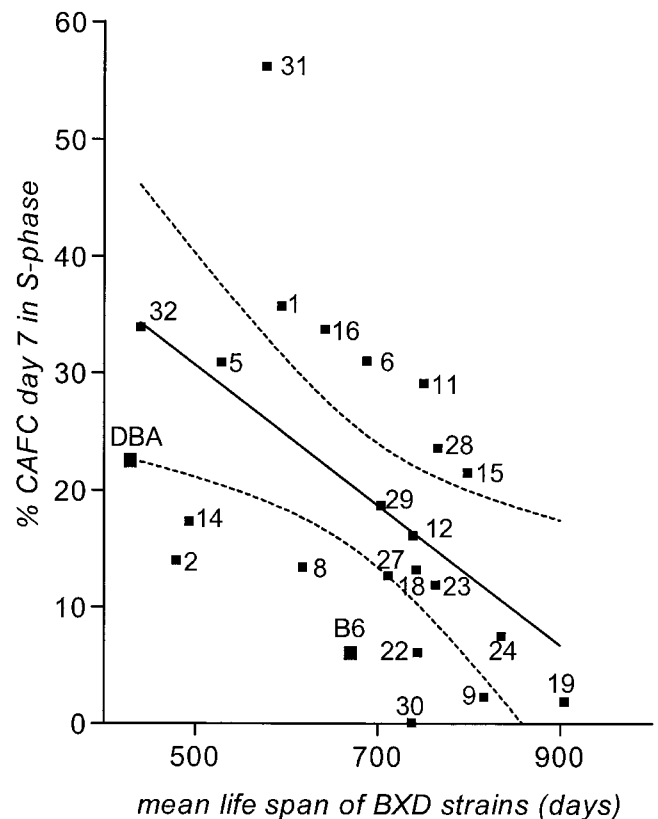


Figure 2. Progenitor cell cycling and mean life span are inversely correlated in BXD recombinant inbred mice. The data as shown in Fig. 1 were related to data obtained by Gelman et al. (19) on the mean life span of 22 BXD strains. A significant negative linear correlation was demonstrated ($Y = 60.605 - 0.06 X$, $r^2 = 0.29$, $P = 0.0093$). The numbers next to each circle refer to the BXD strain numbers. The black squares represent the parental C57BL/6 (B6) and DBA/2 (DBA) mice (49). No life span data were available for BXD strains 13, 20, 21, and 25. The dotted lines represent the 95% confidence intervals.

TABLE 1. Quantitative trait loci most strongly associated with hemopoietic progenitor cell cycling and mean mouse life span in BXD recombinant inbred mice^a

Progenitor cell cycling			Mouse life span		
Locus (chr, cM)	LOD score	Point-wise <i>P</i> value	Locus (chr, cM)	LOD score	Point-wise <i>P</i> value
Ly39 (4, 78.0 cM)	1.8	3.9×10^{-3}	D2Rik63 (2, 69.0 cM)	3.7	3.9×10^{-5}
D7Ncvs52 (7, 6.0 cM)	1.6	6.7×10^{-3}	Ms6hm (4, 40.3 cM)	2.2	1.5×10^{-3}
D9Mit15 (9, 61.0 cM)	1.6	6.1×10^{-3}	D7Ncvs38 (7, 6.0 cM)	3.4	6.5×10^{-5}
D11Ncvs76 (11, 31.0 cM)	3.2	1.3×10^{-4}	D11Rik100 (11, 31.0 cM)	2.1	1.8×10^{-3}

^a Shown are four loci for both progenitor cell cycling and mouse life span that were most strongly associated with each trait. Numbers in parentheses refer to the chromosome number to which a locus maps and to the approximate centiMorgan (cM) position on that chromosome. Note that D7Ncvs52 and D7Ncvs38, and D11Ncvs76 and D11Rik100, map to the same intervals on chromosomes 7 and 11, respectively.

affecting life span. Four regions were identified; two major QTLs on chromosomes 2 and 7, also reaching the genome-wide levels required for suggestive linkage, and two weaker ones on chromosomes 4 and 11 (Table 1). These data were gathered during 1982–1986 and published in 1988, when the mouse genetic map was not dense and mapped traits in the BXD set in particular were sparse. The QTL on chromosome 11 was not detected in the original study because insufficient markers on that chromosome were available at that time (19). In addition, the authors had to omit data from BXD strains 31 and 32 from their analysis since these strains had not been genotyped well enough at that time.

It is striking that of the four loci that we found in each individual search, two were shared by both

traits: one on chromosome 11 (near *D11Ncvs76*) and one on chromosome 7 (near *D7Ncvs38*). Subsequent interval mapping of both progenitor cell cycling and mouse life span resulted in a remarkably similar linkage pattern, with coincident peaks at chromosome 11, 31.0 cM (Fig. 3A) and at chromosome 7, 6.0 cM (not shown).

Figure 3B shows how the BXD strains segregate into the two extreme genotypes for these two loci on chromosomes 7 and 11. C57BL/6 alleles at both *D7Ncvs38* and *D11Ncvs76* were associated with a longer life span (mean of 765 days) and low progenitor cell cycling (9.2%), whereas the corresponding DBA/2 alleles predisposed animals to a 25% shorter life span (mean of 592 days) and high progenitor cycling (32.4%). Linkage to *D2Rik63* and *Ms6hm*, the

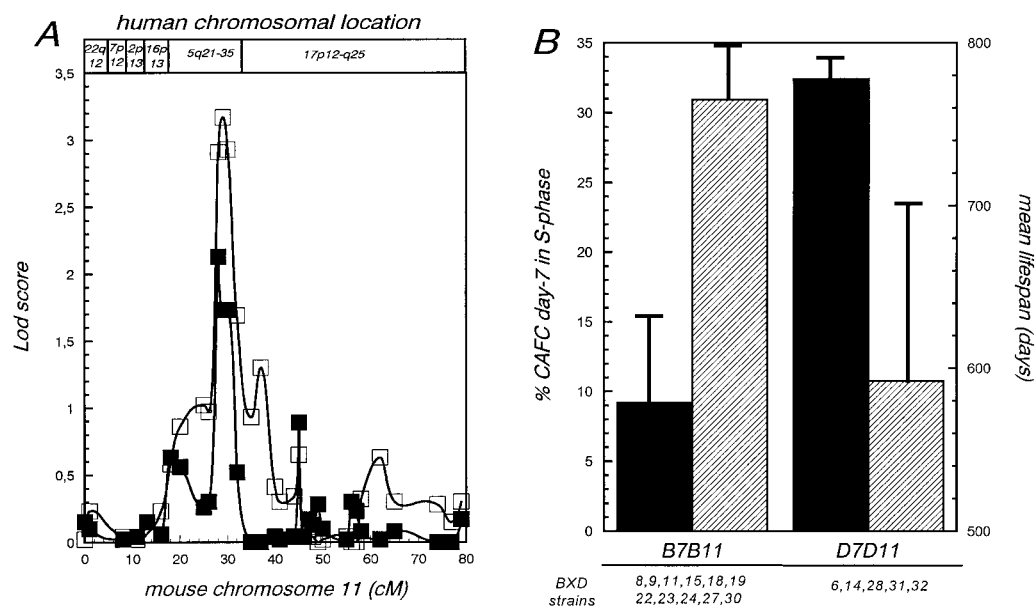


Figure 3. A) QTLs affecting progenitor cell cycling and mouse life span map to the same interval on chromosome 11. LOD score plot showing results of the interval mapping of CAFC day 7 cycling (open squares) and mean life span (closed squares) on chromosome 11. The corresponding map position of orthologous genes in human are shown at the top of the figure. B) Genotypic segregation of BXD strains according to the distribution of C57BL/6 (B) and DBA/2 (D) alleles at *D7Ncvs38* and *D11Ncvs76*. Black bars indicate hemopoietic progenitor cell cycling (left y axis, \pm standard deviation). Hatched bars show strain life span (right y axis, \pm standard deviation). Long-lived strains type B for both loci and have a low percentage of cycling progenitors. Shorter lived strains type D for both loci and have a high percentage of cycling progenitors.

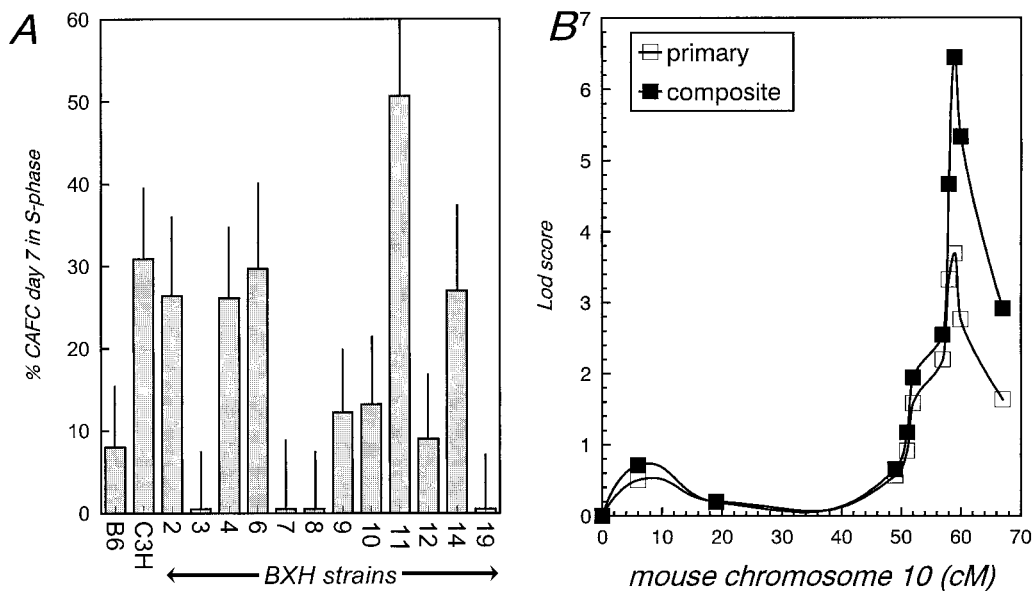


Figure 4. A) Strain distribution pattern for CAFC day 7 cycling in 12 BXH strains. Values for parental C57BL/6 (B6) and C3H/He are indicated. B) LOD score plot showing the results of the primary interval mapping of CAFC day 7 cycling in BXH mice on chromosome 10 (open squares). Results of the composite interval mapping controlling for modifying loci on chromosome 11 are indicated by filled squares.

other two life span QTLs (Table 1), predisposed to a long life span in strains that had the D alleles (i.e., opposite the parental phenotype), and these markers were not associated with cell cycling.

Analysis of variation in hemopoietic progenitor cell cycling in BXH strains

C3H/He mice show an even more pronounced progenitor cell proliferation than do DBA/2 mice (4–6), and therefore we also evaluated variation in cell cycling in BXH recombinant inbred mice (derived from C57BL/6 and C3H/He). **Figure 4A** depicts the strain distribution pattern for the 12 BXH strains. No life span data for BXH strains are available, so we could only perform a linkage analysis for the cycling trait. As described above, a genome-wide search was carried out using the data presented in Fig. 4A. Significant genome-wide linkage (LOD=3.7, point-wise $P=7.3 \times 10^{-5}$, genome-wide $P=0.007$) was found with a locus on chromosome 10, *Iapls2-37*, mapping ~60 cM from the centromere (Fig. 4B). This is very close to the Steel locus encoding the hemopoietic cytokine c-kit ligand (also known as stem cell factor or mast cell growth factor). Since it was obvious from the BXH phenotypes that more than one locus was involved in the variation in cell cycling and because we had obtained sufficient statistical power that allowed us to suspect the involvement of a locus on chromosome 10, we used the composite interval mapping approach, as recently described by Williams et al. (20). In such an analysis, a second search is initiated for loci associated with the phenotypic variation that is unaccounted for by the primary QTL. To do this we performed a second genome-wide search using all BXH data, but now controlling for *Iapls2-37*. Using this approach, link-

age was observed with loci on chromosome 11 (*Iapls1-74*, *Scya3*, and *Xmv42*, peak LOD score 2.8, point-wise P value 0.00036), bracketing the peak shown in Fig. 3A obtained in the BXD set. Thus, we obtained independent evidence of the involvement of a locus on chromosome 11 in progenitor cell cycling (the combined LOD score was 7.34, point-wise P value = 8.37×10^{-7} , genome-wide $P < 0.001$). When we controlled for the loci on chromosome 11, the LOD score for the locus on chromosome 10 in the BXH set greatly improved (to LOD = 6.45, point-wise $P=4.93 \times 10^{-8}$, genome-wide $P < 0.001$, Fig. 4B), again confirming the veracity of the chromosome 11 QTL. We propose to name the QTL on chromosome 7 ‘stem cell proliferation 1’ (*Scp1*), the locus on chromosome 11 *Scp2*, and the locus on chromosome 10, mapped in the BXH set, *Scp3*.

DISCUSSION

Hemopoietic stem cells of different inbred strains of mice demonstrate a genotype-specific proliferative activity that is inversely correlated with organismal life span (5, 6). We have mapped loci associated with cell cycle variation between C57BL/6, DBA/2, and C3H/He mice, and demonstrate that two of these loci also contribute to life span variation in these strains. These results argue compellingly for a causal relationship between hemopoietic cell cycling and mouse life span, and provide evidence for the importance of replicative cycling in the aging process *in vivo*.

Our earlier studies have shown that if highly cycling hemopoietic stem cells of short-lived DBA/2 genotype are put in competition with slowly cycling stem cells of C57BL/6 genotype in the common

environment of embryo aggregation chimeras, mature blood cells of the DBA/2 genotype disappear from the circulation at a time roughly equivalent to the maximal life span of that strain (7). These and other results have led us to argue that true self-renewal of individual hemopoietic stem cells may not exist and that the number of stem cells is finite (23). The aging of stem cells (i.e., decline of stem cell quality) would be dependent on the rate of cycling of these cells, which we have shown to be highly strain dependent and inversely correlated with organismal life span. Stem cells of long-lived C57BL/6, whether measured by long-term repopulating ability (24, 25), cell surface phenotype determined by flow cytometry (26), or using the CAFC assay (5, 27), have not been shown to be detrimentally affected by aging, whereas stem cell activity of shorter lived CBA/J (25) and DBA/2 (5, 27) strains clearly declines with age.

To map loci that contributed to this strain-dependent variation in proliferative activity of stem cells, we used BXD and BXH recombinant inbred mice. The analytical power of using these recombinant inbred strains resides in the fact that the genotype is fixed, so that one can go back to study a different trait in the same genetic background. This is clearly emphasized by our current study, where we compared a strain distribution pattern for cell cycling with life span data obtained 15 years ago (19). This advantage has been underscored by Plomin et al. (28), who have established a BXD recombinant inbred-QTL Cooperative Data Registry that enables comparison of longevity data to other traits reported in the literature concerning the BXD series (28). To date, they have not been able to correlate any of some 137 BXD-phenotypes with longevity (29). In this report we present the first such significant correlation. Our analysis resulted in the identification of four putative intervals associated with cell cycling. It is worth noting that when these were compared with those obtained by searching for life span loci, two of four independently mapped QTLs associated with these traits in BXD mice mapped to the same intervals. The individual QTLs reached the statistical criteria required for suggestive linkage, and combining BXD and BXH data by using composite interval mapping strategies resulted in the identification of a significantly linked QTL on chromosome 11 (20, 21). The strain distribution pattern for stem cell cycling that we present in Fig. 1 is almost an exact mirror image of the pattern reported by Muller-Sieburg (30), where the frequency of long-term culture-initiating cells in BXD strains was measured. At present we have no clear explanation for this finding.

Together with our finding that, in young animals from eight standard inbred strains of mice, progenitor cell cycling and life span are inversely correlated

(6), this *in vivo* study suggests strongly that genes affecting the intrinsic rate of cell cycling also affect the rate of aging of mammalian organisms. The loci we have mapped contain genes that regulate cell cycling in at least one, but potentially more, critical renewing tissues. The nature of these genes remains to be elucidated and is under study. The genomic segment encompassing *D11Ncos76* contains the mouse cytokine cluster (i.e., genes for interleukins 3, 4, 5, 13, and granulocyte-macrophage colony-stimulating factor map here) and is syntenic to human 5q31. Perhaps not coincidentally, we have recently mapped a QTL significantly associated with hemopoietic stem cell (CAFC day 35) frequency to a region of mouse chromosome 18 that is also syntenic to human 5q (6). Deletions of this chromosomal region in humans are associated with the 5q- myelodysplastic syndrome (31–37).

Aging is clearly a multifactorial process (19, 38–42), but our study suggests that, like recent advances made in this field in *Caenorhabditis elegans* and *Saccharomyces cerevisiae* (43, 44), it is open to genetic analysis in mammals. Our findings support a model in which the rate of aging of an organism is partly the result of proliferation kinetics of certain critical tissues/organs. Inherent differences in cell cycle kinetics may determine the speed at which Hayflick's mitotic clock ticks (11, 45) and telomeres shorten (12, 13, 46), but may also alter the rate at which potentially fatal DNA damage accumulates (39, 47, 48). Genetic and/or environmental variations affecting either of these parameters may alter potential life span. **[F]**

This work was supported by funds provided by the Lucille P. Markey Cancer Center, the University of Kentucky Hospital, and the Department of Internal Medicine. G.d.H. is supported by a fellowship awarded by The Netherlands Organization for Scientific Research. The authors thank Dr. Rob Williams for invaluable assistance with MapManager, Dr. Stephen Szilvassy for critically reading the manuscript, and Melissa Flett for statistical analyses.

REFERENCES

1. Rosendaal, M., Hodgson, G. S., and Bradley, T. R. (1979) Organization of haemopoietic stem cells: the generation-age hypothesis. *Cell Tissue Kinet.* **12**, 17–29
2. Van Zant, G. (1984) Studies of hematopoietic stem cells spared by 5-fluorouracil. *J. Exp. Med.* **159**, 679–690
3. Down, J. D., and Ploemacher, R. E. (1993) Transient and permanent engraftment potential of murine hematopoietic stem cell subsets: differential effects of host conditioning with gamma radiation and cytotoxic drugs. *Exp. Hematol.* **21**, 913–921
4. Van Zant, G., Eldridge, P. W., Behringer, R. R., and Dewey, M. J. (1983) Genetic control of hematopoietic kinetics revealed by analyses of allophenic mice and stem cell suicide. *Cell* **35**, 639–645
5. de Haan, G., Nijhof, W., and Van Zant, G. (1997) Mouse strain-dependent changes in frequency and proliferation of hematopoietic stem cells during aging: correlation between lifespan and cycling activity. *Blood* **89**, 1543–1550

6. de Haan, G., and Van Zant, G. (1997) Intrinsic and extrinsic control of hemopoietic stem cell numbers: mapping of a stem cell gene. *J. Exp. Med.* **186**, 529–536
7. Van Zant, G., Holland, B. P., Eldridge, P. W., and Chen, J. J. (1990) Genotype-restricted growth and aging patterns in hematopoietic stem cell populations of allophenic mice. *J. Exp. Med.* **171**, 1547–1565
8. Lansdorp, P. M., Dragowska, W., and Mayani, H. (1993) Ontogeny-related changes in proliferative potential of human hematopoietic cells. *J. Exp. Med.* **178**, 787–791
9. Notaro, R., Cimmino, A., Tabarini, D., Rotoli, B., and Luzzatto, L. (1997) In vivo telomere dynamics of human hematopoietic stem cells. *Proc. Natl. Acad. Sci. U. S. A.* **94**, 13782–13785
10. Wynn, R. F., Cross, M. A., Hatton, C., Will, A. M., Lashford, L. S., Dexter, T. M., and Testa, N. G. (1998) Accelerated telomere shortening in young recipients of allogeneic bone-marrow transplants. *Lancet* **351**, 178–181
11. Hayflick, L. (1965) The limited in vitro lifetime of human diploid cell strains. *Exp. Cell Res.* **37**, 614–636
12. Bodnar, A. G., Ouellette, M., Frolkis, M., Holt, S. E., Chiu, C. P., Morin, G. B., Harley, C. B., Shay, J. W., Lichtsteiner, S., and Wright, W. E. (1998) Extension of life-span by introduction of telomerase into normal human cells. *Science* **279**, 349–352
13. Allsopp, R. C., Vaziri, H., Patterson, C., Goldstein, S., Younglai, E. V., Futcher, A. B., Greider, C. W., and Harley, C. B. (1992) Telomere length predicts replicative capacity of human fibroblasts. *Proc. Natl. Acad. Sci. U. S. A.* **89**, 10114–10118
14. Ploemacher, R. E., van der Sluijs, J. P., van Beurden, C. A., Baert, M. R., and Chan, P. L. (1991) Use of limiting-dilution type long-term marrow cultures in frequency analysis of marrow-repopulating and spleen colony-forming hematopoietic stem cells in the mouse. *Blood* **78**, 2527–2533
15. de Haan, G., Dontje, B., Engel, C., Loeffler, M., and Nijhof, W. (1996) Prophylactic pretreatment of mice with hematopoietic growth factors induces expansion of primitive cell compartments and results in protection against 5-fluorouracil-induced toxicity. *Blood* **87**, 4581–4588
16. Neben, S., Donaldson, D., Sieff, C., Mauch, P., Bodine, D., Ferrara, J., Yetz-Aldape, J., and Turner, K. (1994) Synergistic effects of interleukin-11 with other growth factors on the expansion of murine hematopoietic progenitors and maintenance of stem cells in liquid culture. *Exp. Hematol.* **22**, 353–359
17. Ploemacher, R. E., van der Loo, J. C., van Beurden, C. A., and Baert, M. R. (1993) Wheat germ agglutinin affinity of murine hemopoietic stem cell subpopulations is an inverse function of their long-term repopulating ability *in vitro* and *in vivo*. *Leukemia* **7**, 120–130
18. Manley, K. F. (1993) A Macintosh program for storage and analysis of experimental mapping data. *Mamm. Genome* **4**, 303–313
19. Gelman, R., Watson, A., Bronson, R., and Yunis, E. (1988) Murine chromosomal regions correlated with longevity. *Genetics* **118**, 693–704
20. Williams, R. W., Strom, R. C., and Goldowitz, D. (1998) Natural variation in neuron number in mice is linked to a major quantitative trait locus on Chr 11. *J. Neurosci.* **18**, 138–146
21. Lander, E. S., and Kruglyak, L. (1995) Genetic dissection of complex traits: guidelines for interpreting and reporting linkage results. *Nat. Genet.* **11**, 241–247
22. Churchill, G. A., and Doerge, R. W. (1994) Empirical threshold values for quantitative trait mapping. *Genetics* **138**, 963–971
23. Van Zant, G., de Haan, G., and Rich, I. N. (1997) Alternatives to stem cell renewal from a developmental viewpoint. *Exp. Hematol.* **25**, 187–192
24. Harrison, D. E. (1972) Normal function of transplanted mouse erythrocyte precursors for 21 months beyond donor life spans. *Nature New Biol.* **237**, 220–222
25. Harrison, D. E. (1983) Long-term erythropoietic repopulating ability of old, young, and fetal stem cells. *J. Exp. Med.* **157**, 1496–1504
26. Morrison, S. J., Wandycz, A. M., Akashi, K., Globerson, A., and Weissman, I. L. (1996) The aging of hematopoietic stem cells. *Nat. Med.* **2**, 1011–1016
27. de Haan, G., and Van Zant, G. (1999) Dynamic changes in mouse hematopoietic stem cell numbers during aging. *Blood* In press
28. Plomin, R., McClearn, G. E., Gora-Maslak, G., and Neiderhiser, J. M. (1991) An RI QTL cooperative data bank for recombinant inbred quantitative trait loci analyses. *Behav. Genet.* **21**, 97–98
29. McClearn, G. E. (1997) Prospects for quantitative trait locus methodology in gerontology. *Exp. Gerontol.* **32**, 49–54
30. Muller-Sieburg, C. E., and Riblet, R. (1996) Genetic control of the frequency of hematopoietic stem cells in mice: mapping of a candidate locus to chromosome 1. *J. Exp. Med.* **183**, 1141–1150
31. Boultonwood, J., Fidler, C., Lewis, S., Kelly, S., Sheridan, H., Littlewood, T. J., Buckle, V. J., and Wainscoat, J. S. (1994) Molecular mapping of uncharacteristically small 5q deletions in two patients with the 5q- syndrome: delineation of the critical region on 5q and identification of a 5q- breakpoint. *Genomics* **19**, 425–432
32. Boultonwood, J., Lewis, S., and Wainscoat, J. S. (1994) The 5q- syndrome. *Blood* **84**, 3253–3260
33. Boultonwood, J., Fidler, C., Soularue, P., Strickson, A. J., Kostrzewa, M., Jaju, R. J., Cotter, F. E., Fairweather, N., Monaco, A. P., Muller, U., Lovett, M., Jabs, E. W., Auffray, C., and Wainscoat, J. S. (1997) Novel genes mapping to the critical region of the 5q- syndrome. *Genomics* **45**, 88–96
34. Fairman, J., Chumakov, I., Chinault, A. C., Nowell, P. C., and Nagarajan, L. (1995) Physical mapping of the minimal region of loss in 5q- chromosome. *Proc. Natl. Acad. Sci. U. S. A.* **92**, 7406–7410
35. Willman, C., Sever, C., Pallavicini, M., Harada, H., Tanaka, N., Slovak, M., Yamamoto, H., Harada, K., Meeker, T., List, A., and Taniguchi, T. (1993) Deletion of IRF-1, mapping to chromosome 5q31.1, in human leukemia and preleukemic myelodysplasia. *Science* **259**, 968–971
36. Le Beau, M., Espinosa, R., 3rd, Neuman, W., Stock, W., Roulston, D., Larson, R., Keinanen, M., and Westbrook, C. (1993) Cytogenetic and molecular delineation of the smallest commonly deleted region of chromosome 5 in malignant myeloid diseases. *Proc. Natl. Acad. Sci. U. S. A.* **90**, 5484–5488
37. Zhao, N., Stoffel, A., Wang, P. W., Eisenbart, J. D., Espinosa, R., 3rd, Larson, R. A., and Le Beau, M. M. (1997) Molecular delineation of the smallest commonly deleted region of chromosome 5 in malignant myeloid diseases to 1-1.5 Mb and preparation of a PAC-based physical map. *Proc. Natl. Acad. Sci. U. S. A.* **94**, 6948–6953
38. Campisi, J. (1996) Replicative senescence: an old lives' tale? *Cell* **84**, 497–500
39. Smith, J. R., and Pereira-Smith, O. M. (1996) Replicative senescence: implications for in vivo aging and tumor suppression. *Science* **273**, 63–67
40. Rohme, D. (1981) Evidence for a relationship between longevity of mammalian species and life spans of normal fibroblasts in vitro and erythrocytes in vivo. *Proc. Natl. Acad. Sci. U. S. A.* **78**, 5009–5013
41. Smeal, T., and Guarente, L. (1997) Mechanisms of cellular senescence. *Curr. Opin. Genet. Dev.* **7**, 281–287
42. de Haan G., and Van Zant G. (1998) A putative gene causes variability in lifespan among genotypically identical mice. *Nat. Genet.* **19**, 114–116
43. Kennedy, B. K., and Guarente, L. (1996) Genetic analysis of aging in *Saccharomyces cerevisiae*. *Trends Genet.* **12**, 355–359
44. Kenyon, C. (1996) Ponce d'elegans: genetic quest for the fountain of youth. *Cell* **84**, 501–504
45. Hayflick, L., and Moorhead, P. (1961) The serial cultivation of human diploid cell strains. *Exp. Cell Res.* **25**, 585–621
46. Vaziri, H., Dragowska, W., Allsopp, R. C., Thomas, T. E., Harley, C. B., and Lansdorp, P. M. (1994) Evidence for a mitotic clock in human hematopoietic stem cells: loss of telomeric DNA with age. *Proc. Natl. Acad. Sci. U. S. A.* **91**, 9857–9860
47. Rubin, H. (1997) Cell aging in vivo and in vitro. *Mech. Ageing Dev.* **98**, 1–35
48. Dolle, M. E., Giese, H., Hopkins, C. L., Martus, H. J., Hausdorff, J. M., and Vijg, J. (1997) Rapid accumulation of genome rearrangements in liver but not in brain of old mice. *Nat. Genet.* **17**, 431–434
49. Russel, E. S. (1966) Lifespan and aging patterns. In *Biology of the Laboratory Mouse* (Green, E. L. ed) pp. 511–519, McGraw-Hill Book Company, New York

Received for publication September 29, 1998.
Revised for publication November 23, 1998.